

Anesthesiology
 1999; 91:1861-72
 © 1999 American Society of Anesthesiologists, Inc.
 Lippincott Williams & Wilkins, Inc.

Hemodilution during Venous Gas Embolization Improves Gas Exchange, without Altering \dot{V}_A/\dot{Q} or Pulmonary Blood Flow Distributions

Steven Deem, M.D.,* Steven McKinney, Ph.D.,† Nayak L. Polissar, Ph.D.,‡ Richard G. Hedges, M.S.,§ Erik R. Swenson, M.D.||

Background: Isovolemic anemia results in improved gas exchange in rabbits with normal lungs but in relatively poorer gas exchange in rabbits with whole-lung atelectasis. In the current study, the authors characterized the effects of hemodilution on gas exchange in a distinct model of diffuse lung injury: venous gas embolization.

Methods: Twelve anesthetized rabbits were mechanically ventilated at a fixed rate and volume. Gas embolization was induced by continuous infusion of nitrogen *via* an internal jugular venous catheter. Serial hemodilution was performed in six rabbits by simultaneous withdrawal of blood and infusion of an equal volume of 6% hetastarch; six rabbits were followed as controls over time. Measurements included hemodynamic parameters and blood gases, ventilation-perfusion (\dot{V}_A/\dot{Q}) distribution (multiple inert gas elimination technique), pulmonary blood flow distribution (fluorescent microspheres), and expired nitric oxide (NO; chemoluminescence).

Results: Venous gas embolization resulted in a decrease in

partial pressure of arterial oxygen (P_{aO_2}) and an increase in partial pressure of arterial carbon dioxide (P_{aCO_2}), with markedly abnormal overall \dot{V}_A/\dot{Q} distribution and a predominance of high \dot{V}_A/\dot{Q} areas. Pulmonary blood flow distribution was markedly left-skewed, with low-flow areas predominating. Hematocrit decreased from $30 \pm 1\%$ to $11 \pm 1\%$ (mean \pm SE) with hemodilution. The alveolar-arterial P_{O_2} ($A-aP_{O_2}$) difference decreased from 375 ± 61 mmHg at 30% hematocrit to 218 ± 12.8 mmHg at 15% hematocrit, but increased again (301 ± 33 mmHg) at 11% hematocrit. In contrast, the $A-aP_{O_2}$ difference increased over time in the control group ($P < 0.05$ between groups over time). Changes in P_{aO_2} in both groups could be explained in large part by variations in intrapulmonary shunt and mixed venous oxygen saturation (Sv_{O_2}); however, the improvement in gas exchange with hemodilution was not fully explained by significant changes in \dot{V}_A/\dot{Q} or pulmonary blood flow distributions, as quantitated by the coefficient of variation (CV), fractal dimension, and spatial correlation of blood flow. Expired NO increased with with gas embolization but did not change significantly with time or hemodilution.

Conclusions: Isovolemic hemodilution results in improved oxygen exchange in rabbits with lung injury induced by gas embolization. The mechanism for this improvement is not clear. (Key words: Erythrocytes; red blood cells; MIGET; lung.)

* Assistant Professor of Anesthesiology and Medicine, and Adjunct, Pulmonary and Critical Care, Harborview Medical Center, University of Washington.

† Research Consultant, Pulmonary and Critical Care Medicine, University of Washington.

‡ Affiliate Associate Professor, Department of Biostatistics, University of Washington, and The Mountain Whisper-Light Statistical Consulting, Seattle, Washington.

§ Research Technologist, Pulmonary and Critical Care Medicine, University of Washington

|| Associate Professor of Medicine, Pulmonary and Critical Care, Veterans Affairs Puget Sound Health Care System, University of Washington.

Received from the Departments of Anesthesiology and Medicine, University of Washington, Seattle, Washington. Submitted for publication February 26, 1999. Accepted for publication July 8, 1999. Supported by the American Heart Association—Washington Affiliate, Seattle, Washington, and the National Institutes of Health (HL03796-01 and HL45571), Bethesda, Maryland. Presented at the American Lung Association/American Thoracic Society International Conference, Chicago, Illinois, April 27, 1998.

Address reprint requests to Dr. Deem: Department of Anesthesiology, Box 359724, Harborview Medical Center, 325 Ninth Avenue, Seattle, Washington 98104-2499. Address electronic mail to: sdeem@u.washington.edu

IN previous investigations of hemodilution in rabbits, we found that pulmonary oxygen exchange improved as hematocrit decreased if baseline pulmonary function was normal while carbon dioxide exchange was unaffected.^{1,2} The improvements in oxygen exchange and stability in carbon dioxide exchange were associated with an increase in cardiac output and improved ventilation-perfusion (\dot{V}_A/\dot{Q}) distribution.²

Fractal analysis provides a mathematical model by which to describe organ blood flow distribution, including that of the lung.^{3,4} A fractal structure maintains its form over a magnitude of scales. Both the pulmonary bronchial tract and the pulmonary vasculature exhibit tree-like anatomy, which can be described by a fractal model. Glenny and Robertson³ showed that pulmonary blood flow distribution is best described by a fractal model and that gravity plays a secondary role in blood

flow distribution within the lung. We applied fractal analysis to the study of the effects of hemodilution on pulmonary blood flow distribution in healthy rabbits.² Hemodilution was associated with a reduction in the fractal dimension (D) of pulmonary blood flow and an increase in the spatial correlation of pulmonary blood flow. We hypothesized that these changes in pulmonary blood flow distribution, as a consequence of either decreased blood viscosity or increased availability of nitric oxide (NO), resulted in improved \dot{V}_A/\dot{Q} distribution.

However, in the presence of lung disease, anemia may have a deleterious effect on pulmonary gas exchange. In animals with left lung atelectasis, hemodilution resulted in a relative increase in intrapulmonary shunt, which appeared to be secondary to attenuation of hypoxic pulmonary vasoconstriction (HPV).⁵ Additional studies in isolated rabbit lungs confirmed that anemia has an inhibitory effect on HPV.⁶

Because permissive and intentional hemodilution has become widely accepted and practiced in surgical and other acutely ill patients, it is imperative to understand the effects of acute anemia on pulmonary gas exchange in health and disease. Because the available data show opposite effects of anemia in the normal lung and in the presence of atelectasis, we elected to study the effects of hemodilution in a distinct model of more diffuse lung injury: venous gas embolization. This form of lung injury produces partial pulmonary vascular obstruction, with a resulting increase in areas with high \dot{V}_A/\dot{Q} ratios.⁷ Although we hypothesized that acute hemodilution would result in impairment of gas exchange in this model, in part because of attenuation of the expected increase in cardiac output with anemia caused by pulmonary hypertension and in part because of an increase in shunt and low \dot{V}_A/\dot{Q} caused by impairment of HPV, we were surprised to find the opposite effect. However, we are unable to demonstrate significant changes in \dot{V}_A/\dot{Q} or pulmonary blood flow distributions with hemodilution in this model.

Materials and Methods

After obtaining Animal Care Committee approval, we randomized 12 adult Flemish Giant rabbits, weighing approximately 5 kg each, to either control ($n = 6$) or hemodilution ($n = 6$) groups. After placement of an ear vein catheter, animals were anesthetized with intravenous ketamine and xylazine. A tracheotomy was performed, and the animals were mechanically ventilated

(Siemens Servo 900B; Siemens Elema, Solna, Sweden) in the supine position using 100% oxygen, with a tidal volume of approximately 12 ml^{-1} , and a frequency of approximately 20 breaths/min. Pancuronium, 0.2 mg/kg was administered to allow fixed control of minute ventilation (\dot{V}_E), and infusions of ketamine and xylazine and pancuronium for maintenance of anesthesia and paralysis were begun. A carotid arterial catheter, bilateral jugular venous catheters, and a femoral venous catheter were surgically placed. A thermistor-tipped catheter (Baxter Healthcare Corp., Irvine, CA) was placed in the femoral artery and advanced into the descending aorta for cardiac output measurement. The right jugular venous catheter was advanced into the right ventricle for monitoring of right ventricular pressure and sampling of mixed venous blood gases. Heparin, 200 U/kg, was administered intravenously to prevent thrombosis of the intravascular catheters.

After all surgical procedures were completed, arterial blood gases were obtained, and \dot{V}_E was adjusted to achieve a partial pressure of arterial carbon dioxide (Pa_{CO_2}) of 30–35 mmHg at baseline and fixed for the remainder of the experiment. An intravenous infusion of inert gases (see Inert Gas Analysis) was begun for determination of \dot{V}_A/\dot{Q} distribution using the multiple inert gas elimination technique (MIGET).^{8,9} Mean arterial blood pressure, mean right ventricular pressure (RVP), heart rate, and airway pressures were acquired using a Spacelabs 511 monitor (Hillsboro, OR), and recorded using an A-D converter, data acquisition software (Strawberry Tree Inc., Sunnyvale, CA) and a personal computer (Macintosh Inc., Cupertino, CA).

Cardiac output was measured by thermodilution using a previously described method.^{10–12} Normal saline, 1.0 ml (room temperature), was injected *via* the femoral venous catheter. A change in temperature was measured at the thermistor-tipped intraaortic catheter, and cardiac output was calculated using a 9520A cardiac output computer (American Edwards Laboratory, Irvine, CA). Measurements were taken in triplicate and averaged to give a final value for cardiac output.

Venous and arterial blood gases and mixed expired carbon dioxide were measured using an IL 1620 blood gas machine (Instrumentation Laboratory, Lexington, MA). Expired gas samples were obtained in gas-tight syringes from a 50-ml mixing chamber attached to the expiratory limb of the ventilator circuit and transported immediately to the blood gas machine for analysis. Venous (Cv_{O_2}) and arterial (Ca_{O_2}) oxygen content were measured using an IL 482 cooximeter (Instrumentation

HEMODILUTION AND VENOUS GAS EMBOLIZATION

Laboratory, Lexington, MA). Mixed expired NO was measured continuously using chemoluminescence (Sievers Instruments, Inc., Boulder, CO), with gas sampling from the 50-ml mixing chamber at a rate of 120 ml/min. Hematocrit was measured by centrifugation of duplicate samples.

Baseline physiologic parameters, blood gases, and expired NO were recorded after at least 20 min of inert gas infusion (\dot{V}_A/\dot{Q} and blood flow distribution analyses were not performed at baseline). A continuous infusion of nitrogen was then begun through the left internal jugular vein catheter at a rate of approximately $0.006 \text{ ml} \cdot \text{kg}^{-1} \cdot \text{min}^{-1}$. Arterial blood gases were obtained 15 min after the beginning of the nitrogen infusion and every 5 min thereafter to detect alterations in gas exchange. It became evident in pilot experiments that gas exchange abnormalities began simultaneously with increases in mean RVP, and, subsequently, increases in RVP were used as a marker of significant embolic lung injury. The average time to development of lung injury was approximately 40 min after the beginning of the nitrogen infusion. If there was no evidence of lung injury at 45 min, the nitrogen infusion rate was increased to $0.008 \text{ ml} \cdot \text{kg}^{-1} \cdot \text{min}^{-1}$. Virtually all animals developed signs of embolic lung injury at 1 h.

Five minutes after an increase in RVP of 4 mmHg more than baseline was noted, measurements and samples were taken (time point 1, T1). These included arterial and venous blood gases, hematocrit, arterial lactate, mixed expired partial pressure of arterial oxygen (P_{O_2}), P_{CO_2} , NO, and the hemodynamic data and airway pressures mentioned previously. Fluorescent microspheres were injected intravenously for later determination of regional pulmonary blood flow distribution.

After T1 measurements, animals in the hemodilution group underwent three serial isovolemic hemodilutions, with subsequent measurements and microsphere administration approximately 30 min after completion of each hemodilution (1-h intervals, T2, T3, and T4). Hemodilution was performed by simultaneous withdrawal of blood and infusion of 6% hydroxyethylstarch at equal volumes, with exchanges ranging from 50 to 80 ml over 15 min. During hemodilution and for approximately 15 min afterward, the nitrogen infusion was held and then resumed at the previous rate. This maneuver was performed to avoid excessive hemodynamic depression during periods of acute hemodilution and to ensure that animals did not develop cumulative and fatal lung injury after completing all hemodilutions. Control animals were observed over time, with serial measurements and

microsphere injections at 1-h intervals (T2, T3, and T4). The nitrogen infusion was held for approximately 30 min after each set of measurements to coincide with the period during which it was held in those animals undergoing hemodilution. Expired \dot{V}_E was measured at the conclusion of the experiments using a sidestream spirometer (Datex Medical Instruments, Tewksbury, MA), after which animals were killed by a combination of an overdose of ketamine and exsanguination.

Blood samples for analysis of plasma lactate were spun in a microcentrifuge at 12,000 rpm for 20 s. One milliliter of plasma was drawn and frozen at -4°C for later analysis. Lactate levels were assayed using a YSI 1500 Sport Lactate Analyzer (Yellow Springs Instrument Co., Yellow Springs, OH).

Calculations

Carbon dioxide production ($\dot{V}CO_2$) was calculated from the volume and concentration of expired carbon dioxide (using appropriate temperature and humidity corrections) and normalized for body weight. NO output ($\dot{V}NO$) was calculated from the corrected expired \dot{V}_E and the concentration of NO in the expired gas. The fraction of physiologic dead space ($V_D/V_{T \text{ Bohr}}$) was calculated using the Enghoff modification of the Bohr equation and reported as a percentage. Oxygen extraction ratio (O_2ER) was calculated as the ratio of $Ca-v_{O_2}$ to Ca_{O_2} and reported as a fraction. Alveolar P_{O_2} (used to calculate the alveolar-arterial P_{O_2} difference [$A-aP_{O_2}$]) was calculated using the alveolar gas equation.

Inert Gas Analysis

Six inert gases (ethane, halothane, sulfur hexafluoride [SF6], cyclopropane, diethyl ether, and acetone) were dissolved in 5% dextrose solution and infused continuously at 0.7 ml/min. Duplicate arterial and venous blood samples (1 ml) and mixed expired gas samples were obtained at each measurement point; blood and gas samples were drawn simultaneously over approximately 30 s, with a total time for duplicate samples of approximately 2 min. Expired gas samples were stored at 40°C before analysis to avoid water condensation and loss of soluble gases. Concentrations of inert gases were measured using a gas chromatograph (Varian 3300, Walnut Creek, CA) equipped with a flame ionization detector and electron capture detector. The gas extraction method of Wagner *et al.*^{8,13} was used to determine inert gas tensions and solubilities in the blood samples.

The multiple inert gas elimination technique analysis was performed on five control animals and six hemodi-

lution animals postembolization (one control animal was excluded from the analysis because of technical difficulties with the inert gas infusion). Inert gas exchange was assessed by changes in the ventilation and perfusion distributions predicted by the 50-compartment model of Wagner *et al.*^{8,13} Inert gas shunt (Q_S/Q_T); inert gas dead space ($V_D/V_{T \text{ MIGET}}$); perfusion and ventilation distributions to areas of low, mid, and high \dot{V}_A/\dot{Q} ; and log standard deviations of the perfusion ($\log SD_Q$) and ventilation ($\log SD_V$) distributions were calculated from the 50-compartment model. Global \dot{V}_A/\dot{Q} heterogeneity was also assessed using the dispersion index ($\text{Disp } R^*E^*$), derived from the retention (R) and excretion (E) data and corrected for dead space.⁹ Data were averaged from the duplicate samples and are presented as the mean \pm SE for each group. If the sums of squares for an individual data set was greater than 5.0, these data were omitted from the final analysis. This resulted in elimination of only two data sets.

Fluorescent Microsphere Analysis

Fluorescent microspheres of four different colors were kept under ultrasonic agitation (Branson 1200; Branson Cleaning Equipment Co., Shelton, CT) until drawn into a syringe immediately before injection. Each injection contained approximately 3.3 million microspheres of one color in 1 ml, which was calculated to give sufficient resolution based on previously published works.¹⁴⁻¹⁶

After killing at the conclusion of the experiment, a median sternotomy was performed, the pulmonary artery was cannulated, and the left ventricle was opened. The lungs were flushed with 37°C saline containing 2% dextran for 5 min at 150 ml/min. The lungs were then dissected from the chest, the heart and extraneous tissue were removed, and the lungs were suspended and re-inflated at 20 cm H₂O for two days to dry. The dried lungs were encased in blocks of foam sealant and sliced perpendicular to the cranial-caudal axis every 5 mm. The lung slices were placed in a jig with a grid of 6 mm diameter circular holes placed 1 cm at the center. A core of lung tissue was removed from each hole and the piece was given x , y , and z coordinates. The core pieces (approximately 200/lung) were weighed, coded for any airway or residual blood content, and placed in numbered vials. The vials were filled with 1 ml 2-ethoxyethyl acetate to dissolve the microspheres over 24 h, and the solvent was transferred to cuvettes and read for fluorescence (Perkin-Elmer LS50B; Perkin-Elmer Inc., Norwalk, CT) using emission and excitation wavelengths determined by standards containing all four colors. For each

color, the fluorescence of each piece was converted to weight-normalized relative blood flow by dividing by the weight of the individual piece and by the mean fluorescence across all pieces. The resulting normalized flows have a mean of 1.00 for each color.

Fluorescent microsphere analysis was performed on all rabbits postembolization. Heterogeneity of pulmonary blood flow was characterized by calculating the CV of weight-normalized relative blood flow (CV_Q) at each measurement point for each rabbit. The skewness of blood flow (Skewness_Q) was calculated in a similar fashion. Microsphere data were also analyzed using simple linear regression models for flow in relation to linear spatial dimensions X (transverse, right to left), Y (coronal, ventral to dorsal), Z (sagittal, cranial to caudal) and Dh (distance from the hilum, expressed as $[(x - x_h)^2 + (y - y_h)^2 + (z - z_h)^2]^{0.5}$, where x_h , y_h , and z_h are the coordinates of the hilum of each lung [left or right]), to characterize the distribution of pulmonary blood flow across the lung.^{16,17} We analyzed blood flow in the transverse, or x -axis in relation to the orientation of the individual lungs. Thus, rather than characterizing flow in terms of right to left across both lungs, we characterized flow from lateral to medial for each lung and pooled these data.

Pulmonary blood flow heterogeneity was also expressed in terms of D, a measure that does not depend on piece size.³ (See Appendix for detailed description of methods for calculation of D). Finally, characterization of temporal flow patterns and their spatial location within the lung was performed by obtaining weight-normalized relative flow values from all possible neighboring piece pairs within the lung. A correlation coefficient, characterized as the value ρ was then calculated using the Pearson product moment correlation.¹⁸

Statistical Analysis

All data are presented as the mean \pm SE at baseline and the four measurement points (T1-T4) postembolization. Physiologic data were analyzed using the Student t test to detect differences between groups at baseline and T1, and repeated-measures analysis of variance to detect differences between groups over time (T1-T4) using the software package StatView (Abacus Concepts, Berkeley, CA). In this analysis, the treatment group was a between-subject grouping factor, and time was a within-subject repeating factor. This methodology provides a test for the difference in mean values between the two groups over time. A mean difference between groups that changes substantially over time is likely to be statistically

HEMODILUTION AND VENOUS GAS EMBOLIZATION

significant, and it is the P value for this test that is reported.

Because there was a nonsignificant difference in Pa_{O_2} at T1 between groups, we performed additional *post hoc* analysis to control for the effect of this difference on Pa_{O_2} over time or with hemodilution. The Pa_{O_2} value at T1 was subtracted from values at T4 for both groups (T4 - T1). A multiple-regression model was then fitted using three independent variables: baseline Pa_{O_2} , group (a dichotomous indicator variable), and the interaction product of group and T1 Pa_{O_2} ($\text{Grp_T1Pa}_{\text{O}_2}$) as independent variables; T4-T1 was the dependent variable. The significance of the difference between groups in the change in Pa_{O_2} was determined by evaluating the coefficient and P value for the interaction term $\text{Grp_T1Pa}_{\text{O}_2}$.

For MIGET data, differences between groups at T1 were tested using the Student t test, and differences over time or with hemodilution were tested using repeated-measures analysis of variance.

A multiple-regression model was used to determine the variance in Pa_{O_2} explained by other physiologic and MIGET-derived variables. The data from both groups were pooled across all times for the analysis. Pooling provided a large sample size and allowed us to investigate the interaction of the treatment group and time.

Fluorescent microsphere data were used to detect changes in regional pulmonary blood flow between groups over time. The individual regression slopes for the spatial dimensions X, Y, Z, and Dh, the individual CV_{Q} , and $\text{Skewness}_{\text{Q}}$ were compared using repeated-measures analysis of variance, as were changes in D and spatial correlation ρ . T1 differences between groups were analyzed using an unpaired Student t test. Data are presented as the mean \pm SE for each group. For analysis of the D of pulmonary blood flow, the slope of D *versus* time was calculated for each rabbit, and the mean slope for each group was compared to zero using a single-sample t test to detect nonzero trends over time. Similarly, for analysis of temporal and spatial correlation of blood flow, the slope of ρ *versus* time was calculated for each rabbit and the mean slope for each group compared to zero using a single-sample t test to detect nonzero trends over time. A P value < 0.05 was accepted as statistically significant for all analyses.

Results

Physiologic Variables

Baseline physiologic parameters were similar between groups. Baseline Pa_{O_2} was 502 ± 15 mmHg and 481 ± 14

mmHg in control and anemic groups, respectively, and Pa_{CO_2} was 32.4 ± 6.5 and 34.1 ± 2.9 mmHg. Postembolization, there were no significant differences in physiologic parameters between groups (table 1). Hematocrit decreased from $30 \pm 1\%$ to a nadir of $11 \pm 1\%$ with serial hemodilution (table 1). Hematocrit decreased slightly in the control animals because of subsequent blood draws. RVP was similar between groups at baseline (5 ± 0.3 mmHg, control, 6 ± 0.7 mmHg, anemic), and increased to 12 ± 3 and 14 ± 2 mmHg, respectively, postembolization. RVP and mean arterial pressure did not differ significantly between groups over time or with hemodilution (table 1). In contrast to our previous findings in healthy, anesthetized rabbits,^{1,2} cardiac output (Q) did not increase with hemodilution, which probably reflected the effect of pulmonary and right ventricular hypertension induced by gas embolization.

At T1, animals in both groups had an increased A-a P_{O_2} difference and hypercapnia with respiratory acidosis (table 1); the differences between groups were not statistically significant. Hemodilution resulted in an improvement in oxygen exchange, with an increase in Pa_{O_2} and a decrease in the A-a P_{O_2} difference (table 1). This was in contrast to the control group, which exhibited a small decrease in oxygen exchange over time ($P < 0.05$ for Pa_{O_2} and A-a P_{O_2} between groups). The difference in Pa_{O_2} at T4 remained statistically significant when T1 Pa_{O_2} was controlled using linear regression ($P = 0.03$ between groups). Because of the nonsignificant differences at T1 between groups, the improvement in Pa_{O_2} with hemodilution is best illustrated by the change in Pa_{O_2} from T1 (fig. 1). There was a trend toward reduced mixed venous oxygen tension (Pv_{O_2}) with hemodilution, but Pa_{CO_2} and mixed venous carbon dioxide tension (Pv_{CO_2}) were not affected significantly by time or hemodilution (table 1). Venous gas embolization resulted in a large $\text{VD/VT}_{\text{Bohr}}$ (table 1), which did not change significantly with time or hemodilution. Serum lactate levels increased slightly over time, but did not differ significantly between groups (table 1).

$\dot{\text{V}}\text{NO}$ was similar in both groups at baseline and increased at the first embolization point (T1; fig. 2). The difference between baseline and T1 $\dot{\text{V}}\text{NO}$ was statistically significant only for anemic animals ($P < 0.0001$) or when data from control and anemic animals were combined ($P = 0.002$). $\dot{\text{V}}\text{NO}$ remained stable over time in the control group; there was a trend toward decreased $\dot{\text{V}}\text{NO}$ with hemodilution, although the difference between groups over time was only marginally significant ($P = 0.07$; fig. 2).

Table 1. Measured and Calculated Physiologic Variables Postembolization

	Group	T1	T2	T3	T4	P
Hct (%)	C	32 ± 1	29 ± 1	26 ± 1	27 ± 1	<0.0001
	A	30 ± 1	21 ± 1	15 ± 1	11 ± 1*	
MAP (mmHg)	C	93 ± 6	90 ± 3	91 ± 6	76 ± 9	0.65
	A	100 ± 14	88 ± 5	83 ± 6	68 ± 8	
RVP (Torr)	C	12 ± 3	8 ± 1	10 ± 2	10 ± 1	0.41
	A	14 ± 2	12 ± 1	11 ± 1	13 ± 2	
Q (l/min)	C	0.58 ± 0.22	0.54 ± 0.08	0.52 ± 0.09	0.53 ± 0.07	0.51
	A	0.55 ± 0.02	0.49 ± 0.03	0.58 ± 0.03	0.58 ± 0.07	
pH _a	C	7.32 ± 0.05	7.24 ± 0.01	7.22 ± 0.02	7.17 ± 0.05	0.28
	A	7.25 ± 0.02	7.23 ± 0.02	7.26 ± 0.03	7.17 ± 0.04	
Pa _{CO₂} (mmHg)	C	48.0 ± 7.8	52.2 ± 2.9	55.2 ± 4.4	65.6 ± 8.9	0.27
	A	59.7 ± 2.9	63.7 ± 5.1	56.7 ± 6.1	67.5 ± 5.5	
Pa _{O₂} (mmHg)	C	391 ± 76	371 ± 54	337 ± 60	349 ± 67	0.04
	A	268 ± 61	394 ± 34	428 ± 17	334 ± 35†	
A-aP _{O₂} difference (mmHg)	C	265 ± 69	281 ± 54	311 ± 56	289 ± 60	0.03
	A	375 ± 61	245 ± 34	218 ± 12.8	301 ± 33†	
Pv _{O₂} (mmHg)	C	47 ± 2	48 ± 2	50 ± 4	48 ± 2	0.05
	A	42 ± 2	45 ± 2	42 ± 2	36 ± 3	
Pv _{CO₂} (mmHg)	C	53.4 ± 8.6	60.4 ± 6.0	64.0 ± 3.4	72.5 ± 8.5	0.48
	A	64.0 ± 3.9	66.5 ± 6.4	64.0 ± 4.4	72.4 ± 6.6	
V _{CO₂} (ml · kg ⁻¹ · min ⁻¹)	C	3.33 ± 0.52	4.35 ± 0.56	3.76 ± 0.63	4.57 ± 0.32	0.05
	A	3.35 ± 0.34	4.45 ± 0.26	5.58 ± 0.56	4.17 ± 0.16	
V _D /V _{TBohr}	C	0.68 ± 0.08	0.67 ± 0.04	0.72 ± 0.06	0.71 ± 0.04	0.57
	A	0.82 ± 0.01	0.77 ± 0.03	0.66 ± 0.07	0.82 ± 0.03	
O ₂ ER	C	0.32 ± 0.05	0.36 ± 0.04	0.34 ± 0.03	0.38 ± 0.03	0.003
	A	0.39 ± 0.03	0.40 ± 0.04	0.45 ± 0.03	0.59 ± 0.04†	
Lactate (arterial) (mM)	C	4.48 ± 1.22	3.81 ± 1.06	4.34 ± 0.83	5.77 ± 1.31	0.67
	A	3.29 ± 0.94	2.91 ± 0.42	2.75 ± 0.45	4.58 ± 1.10	

Values are mean ± SE; n = 6 in each group.

C = control; A = anemic (hemodilution); T1–T4 = approximately 1-hour time intervals beginning with gas embolization and associated with different levels of hemodilution in group A; O₂ER = oxygen extraction ratio; P values = significance of the difference in mean values between groups over time as detected by repeated measures ANOVA; Hct = hematocrit.

\dot{V}_A/\dot{Q} Distribution (MIGET)

Inert gas analysis revealed a relatively small \dot{Q}_S/\dot{Q}_T and V_D/V_T MIGET, but markedly abnormal overall \dot{V}_A/\dot{Q} (Disp [R²-E*]; table 2). Ventilation was skewed toward areas of high \dot{V}_A/\dot{Q} and perfusion toward areas of low \dot{V}_A/\dot{Q} , as illustrated in the data from a representative control animal at T1 (fig. 3). There was a trend toward increased \dot{Q}_S/\dot{Q}_T in control animals from T1–T3, whereas it remained stable in anemic animals until T4, when it increased from 0.05 to 0.10. Dispersion decreased in both groups from T1–T3 and then increased in anemic animals at T4. However, none of the changes with time or hemodilution in MIGET-derived parameters reached statistical significance. Likewise, there were no changes in ventilation and perfusion distributions to areas of low, mid, and high \dot{V}_A/\dot{Q} with time or hemodilution (data not shown).

\dot{Q}_S/\dot{Q}_T and Sv_{O₂} explained 60% (r² = 0.60) of the variation in Pa_{O₂} as the dependent variable in a regression analysis that pooled observations across the two

treatment groups and the four times of assessment. Other factors, including \dot{V}_A/\dot{Q} dispersion, explained very little of the Pa_{O₂} variation. The effects of \dot{Q}_S/\dot{Q}_T and Sv_{O₂} on Pa_{O₂} appeared to be independent of time, group, and time-by-group interaction.

Pulmonary Blood Flow Distribution (Microspheres)

Microsphere analysis revealed a large CV_Q during gas embolization, and blood flow was markedly skewed with most lung pieces exhibiting very low flow. This is exemplified in data from the same control animal at T1 shown previously (fig. 4). Although there was a slight trend toward reduced CV_Q and Skewness_Q with hemodilution, the difference between control and anemic animals was not statistically significant (table 3).

The D of pulmonary blood flow was higher at T1 in anemic versus control rabbits (P < 0.05), but the difference between groups remained constant over time or hemodilution (table 3). The mean D for both groups combined at T1 was 1.27 ± 0.02. Spatial correlation of

HEMODILUTION AND VENOUS GAS EMBOLIZATION

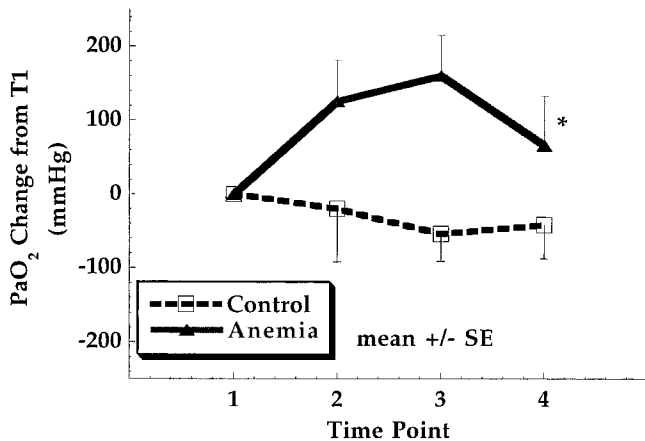


Fig. 1. Change in PaO₂ from T1 in control and anemic groups. * $P < 0.05$ for difference between groups over time.

pulmonary blood flow as quantified by ρ did not differ between groups at T1 or over time (table 3).

Blood flow along the spatial dimensions X, Y, Z, and Dh revealed higher flow to dorsal lung pieces (y -axis, table 3) with a significant correlation of blood flow with this dimension ($r^2 = 0.15$, $P < 0.001$, all animals at T1). Although there was a trend toward redistribution of blood flow toward ventral lung with hemodilution, there were no significant differences in blood flow along any spatial axis between groups and no significant changes with time or hemodilution (table 3).

Discussion

Venous gas embolization in rabbits resulted in a gas exchange abnormality characterized by a large V_D/V_T Bohr, a wide \dot{V}_A/\dot{Q} dispersion, and a relatively small Q_s/Q_T (tables 1 and 2). These changes were associated with markedly skewed blood flow distribution, with the majority of the lung exhibiting low-flow conditions (fig. 4). Hemodilution in the presence of venous gas embolization resulted in improved oxygen exchange (increased PaO₂ and decreased A-aPO₂ difference) in comparison with controls with gas embolization followed-up during an equivalent time interval. The improvement in oxygen exchange was most notable down to a hematocrit of approximately 15%, with further hemodilution to a hematocrit of approximately 11% resulting in little change in PaO₂ or A-aPO₂ difference (fig. 1, table 1). The improvement in oxygen exchange was not associated with significant changes in overall \dot{V}_A/\dot{Q} distribution (table 2), or pulmonary blood flow distribution (table 3), although subtle trends in these distributions with hemodilution

were noted. Indeed, changes in Q_s/Q_T and SvO₂ explained 60% of the observed change in PaO₂ in a multiple-regression model. Because the experiments were conducted at a fraction of inspired oxygen (FiO₂) of 1.0, it is not surprising that addition of other MIGET-derived variables did not strengthen the regression model, given that changes in \dot{V}_A/\dot{Q} distribution would be expected to have little effect on PaO₂ at this FiO₂.

Limitations of the Study

One limitation of this study is the small sample size. A number of the nonsignificant differences between treatment groups may hide some large true differences. For example, for Q_s/Q_T at T4, the differences between means equals 0.02 (control vs. anemia), but the 95% confidence interval for the difference is -0.12 to 0.16 , which includes the possibility of a substantial true difference. However, this lack of power to detect differences in some variables does not negate the significance of differences between groups when found.

Discussion of the Model

This model of venous gas embolization (continuous infusion of small bubbles) may be dissimilar to cases of air embolization in the clinical setting. In the latter case, emboli may be more likely to enter the circulation in bolus fashion, to be larger, and to produce cardiovascular collapse and more focal pulmonary perfusion abnormalities.¹⁹ Extrapolation of the current data to clinical management is therefore difficult.

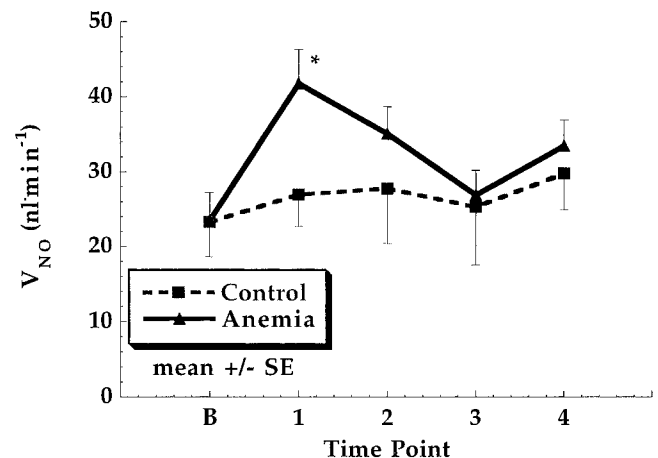


Fig. 2. Expired nitric oxide output (\dot{V}_{NO}) in control and anemic groups at baseline and at embolization times T1-T4. * $P < 0.0001$ for differences between \dot{V}_{NO} at baseline and T1 in the anemic group.

Table 2. \dot{V}_A/Q Distributions (MIGET) Postembolization

	Group	T1	T2	T3	T4	P
Q_s/Q_t	C	0.07 ± 0.03	0.09 ± 0.03	0.16 ± 0.08	0.12 ± 0.05	0.37
	A	0.06 ± 0.03	0.06 ± 0.02	0.05 ± 0.03	0.10 ± 0.04	
V_D/V_T	C	0.30 ± 0.04	0.35 ± 0.03	0.32 ± 0.03	0.29 ± 0.03	0.97
	A	0.30 ± 0.03	0.36 ± 0.02	0.31 ± 0.04	0.30 ± 0.05	
Log SD_V	C	1.1 ± 0.1	1.3 ± 0.04	1.7 ± 0.6	1.3 ± 0.1	0.20
	A	1.3 ± 0.1	1.4 ± 0.1	1.1 ± 0.1	1.6 ± 0.1	
Log SD_Q	C	2.0 ± 0.2	1.7 ± 0.1	1.8 ± 0.3	1.8 ± 0.1	0.90
	A	1.9 ± 0.2	1.9 ± 0.1	1.9 ± 0.1	2.0 ± 0.1	
Dispersion (R^*-E^*)	C	37.6 ± 7.8	30.6 ± 3.5	33.4 ± 7.0	32.5 ± 3.9	0.38
	A	38.1 ± 4.2	37.1 ± 3.1	27.7 ± 4.6	39.4 ± 1.6	

Values are mean ± SE.

C = control (n = 5); A = anemic (hemodilution) (n = 6); T1-T4 = approximately 1-hour time intervals beginning with gas embolization and associated with different levels of hemodilution in group A; P values = significance of the difference in mean values between groups over time as detected by repeated measures ANOVA.

We chose venous gas embolization as a model for study of the effects of anemia on gas exchange because of its relative stability and titratability over time in comparison with other models of lung injury. In addition, we thought that hemodilution-induced anemia might have deleterious effects on gas exchange in this model because of the effects of reduced blood viscosity on the distribution of blood flow in a partially obstructed vascular tree. We followed the protocol for venous gas embolization previously used by Hlastala *et al.*,⁷ with three exceptions

1. We forced the gas through smaller tubing (PE 20 vs. PE 25) based on the smaller subject size in our study (rabbits vs. dogs).
2. Based on pilot studies, we used a slower rate of gas infusion than that used by Hlastala *et al.*⁷ and others to avoid severe hemodynamic embarrassment and to

ensure a longer study duration than that used by Hlastala *et al.*⁷ (4 h vs. 2.5 h).

3. We used intermittent gas infusion rather than continuous infusion to allow some hemodynamic recovery between measurement periods. Again, this step was taken to ensure survival of the animals for the duration of the study. Because we used a lower rate of infusion (and perhaps because of smaller bubble size), a longer initial period of gas infusion was necessary before hemodynamic and gas exchange abnormalities were evident (30–60 min vs. 5 min).

Hlastala *et al.*⁷ suggested that small-bubble embolization resulted in initial obstruction of large pulmonary arteries, after which the bubble would decrease and slip more distally in the pulmonary artery. They found that

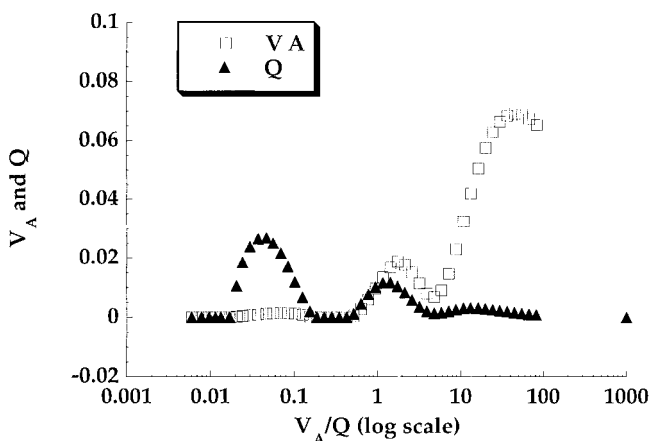


Fig. 3. \dot{V}_A/Q distribution in a representative control animal after embolization (time T1). Perfusion distribution is bimodal with a large component to areas of high \dot{V}_A/Q .

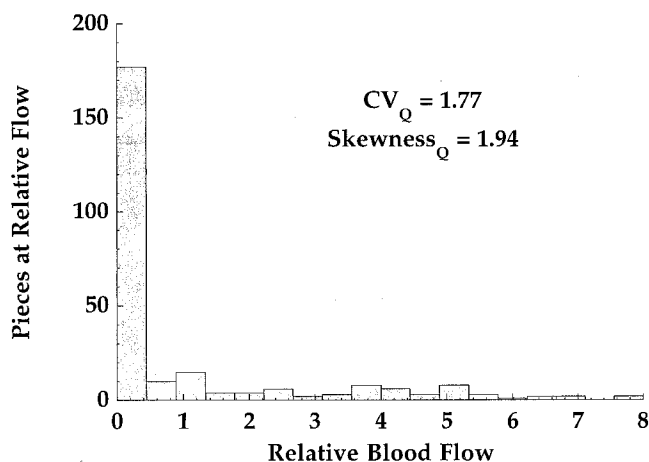


Fig. 4. Pulmonary blood flow distribution in a representative control animal after venous gas embolization (time T1). Blood flow is skewed toward areas of low flow, with a broad distribution to other pieces. CV_Q = coefficient of variation of blood flow.

HEMODILUTION AND VENOUS GAS EMBOLIZATION

Table 3. Pulmonary Blood Flow Distribution Variables (microspheres) Postembolization

Variable	Group	T1	T2	T3	T4	P
CV _Q	C	1.26 ± 0.28	1.28 ± 0.21	1.59 ± 0.30	1.14 ± 0.22	0.35
	A	1.76 ± 0.30	1.51 ± 0.14	1.30 ± 0.23	1.26 ± 0.26	
Skewness _Q	C	1.34 ± 0.40	0.97 ± 0.40	1.80 ± 0.54	1.31 ± 0.35	0.43
	A	2.25 ± 0.15	1.80 ± 0.28	1.65 ± 0.48	1.61 ± 0.52	
D	C	1.22 ± 0.02*	1.23 ± 0.03	1.25 ± 0.2	1.24 ± 0	0.56
	A	1.32 ± 0.02	1.29 ± 0.02	1.29 ± 0.03	1.30 ± 0.10	
ρ	C	0.52 ± 0.04	0.52 ± 0.05	0.52 ± 0.04	0.53 ± 0.04	0.79
	A	0.41 ± 0.07	0.48 ± 0.13	0.42 ± 0.07	0.46 ± 0.07	
Spatial axes						
X (Lat→Med slope)	C	0.065 ± 0.029	0.003 ± 0.041	0.052 ± 0.084	0.087 ± 0.022	0.23
	A	0.069 ± 0.051	0.080 ± 0.028	0.010 ± 0.049	0.027 ± 0.036	
Y (V→D slope)	C	0.292 ± 0.085	0.299 ± 0.068	0.350 ± 0.081	0.261 ± 0.043	0.12
	A	0.380 ± 0.082	0.316 ± 0.099	0.230 ± 0.108	0.270 ± 0.087	
Z (Cr→Cau slope)	C	-0.073 ± 0.053	-0.098 ± 0.034	-0.117 ± 0.028	-0.078 ± 0.039	0.74
	A	-0.107 ± 0.015	-0.130 ± 0.015	-0.107 ± 0.027	-0.067 ± 0.031	
D _h (slope)	C	-0.090 ± 0.061	-0.065 ± 0.053	-0.117 ± 0.059	-0.090 ± 0.048	0.61
	A	-0.131 ± 0.034	-0.106 ± 0.027	-0.097 ± 0.028	-0.071 ± 0.044	

Values are mean ± SE.

C = control; A = anemic (hemodilution); n = 6 in both groups; T1–T4 = approximately 1-hour time intervals beginning with gas embolization and associated with different levels of hemodilution in group A; P values = significance of the difference in mean values between groups over time as detected by repeated measures ANOVA; CV_Q = coefficient of variation of blood flow; D = fractal dimension of blood flow; ρ = spatial correlation of blood flow; Lat→Med = lateral to medial (for individual lungs); V→D = ventral to dorsal; Cr→Cau = cranial to caudal; D_h = distance from the hilum.

* P < 0.05 between groups at T1.

gas exchange abnormalities reached steady state after approximately 15 min of embolization. Because of the differences in our protocol, it is possible that the animals in our study were not at steady state at the time of measurements. This may explain the relatively large variability in gas exchange parameters among animals. However, animals in both the study and the control groups were treated identically, which should control for any variability in the degree of vascular obstruction at the time of measurement. Hlastala *et al.*⁷ also found that there was evidence of pulmonary edema (increased wet/dry ratios) after 2.5 h of venous gas embolization, and other investigators^{20–22} also documented pulmonary edema in association with venous gas infusion. Although we did not perform wet/dry ratios in our animals, the development of occult pulmonary edema may have been responsible for the relative decrease in the beneficial effects of hemodilution on gas exchange over time (fig. 1) and the increase in Q_S/Q_T and heterogeneity at the last hemodilution (table 2). Anemia has an adverse effect on HPV,^{3,6} and the attenuation of HPV in the presence of increasing pulmonary edema, shunt, and low \dot{V}_A/\dot{Q} may have masked any salutary effects of anemia on pulmonary vascular obstruction. Q_S/Q_T caused by the development of atelectasis over time might be more pronounced in anemic animals for the same reason.

Like Hlastala *et al.*,⁷ we found that venous gas embolization resulted in a relatively small Q_S/Q_T and a large V_D/V_T Bohr (tables 1 and 2). V_D/V_T MIGET was not increased compared with normal controls from previous work,² but \dot{V}_A/\dot{Q} distributions were markedly skewed to regions of high \dot{V}_A/\dot{Q} . The absence of high V_D/V_T MIGET and the predominance of high \dot{V}_A/\dot{Q} ratios may be an averaging effect of parallel dead space in the presence of series dead space.⁷ In addition, gas embolization may not produce complete vascular obstruction, particularly if bubbles are lodged in lung units fed by multiple microvessels.⁷

The marked skewness of pulmonary blood flow distribution as measured by fluorescent microsphere analysis, with most lung exhibiting low flow (fig. 4) supports the presence of diffuse vascular obstruction in this model. There was considerable interanimal and between-measurement variability, however, suggesting some evolution in bubble size and distribution over time.

Given the derivation of D (one – slope of the log-log plot of the CV_Q vs. piece size; Appendix), the lower boundary for D is 1.0. A D of 1.0 therefore implies complete correlation of blood flow between neighboring pieces, whereas a D of 1.5 suggests that flow is randomly distributed among neighboring pieces.⁴ The derivation of D thus allows comparison of the heterogeneity of organ blood flow that is independent of the species, organ, or piece size analyzed. In the current

study, the highly linear trends in the plots of $\log(CV_Q)$ versus $\log(\text{conglomerate piece size})$ used to determine D is consistent with pulmonary blood flow distribution in the rabbit that is fractal in nature in the presence of gas embolism.^{3,4} D was higher in the presence of venous gas embolization than in a previously published result from rabbits with normal lungs and a comparable hematocrit (1.27 ± 0.02 vs. 1.21 ± 0.05).² The value of 1.27 for D suggests that pulmonary blood flow distribution has greater local heterogeneity with embolization than in the normal rabbit lung, although the differences are small. Likewise, the spatial correlation of pulmonary blood flow as quantitated by ρ is slightly lower in the current study than in normal rabbits (0.47 ± 0.04 vs. 0.50 ± 0.03).² These observations emphasize the importance of structural characteristics of the lung in determining pulmonary blood flow distribution.

Anemia and Lung Injury

In rabbits with normal lungs, acute isovolemic anemia results in improvements in gas exchange in association with reduced \dot{V}_A/\dot{Q} heterogeneity, a reduced D of pulmonary blood flow, and increased spatial correlation of pulmonary blood flow.² These effects are probably mediated by the reduced blood viscosity associated with anemia, with the possible contribution of increased available NO and its resulting vascular effects.^{2,6} In the presence of lung injury, however, some studies have not found salutary effects of anemia on gas exchange. Bishop and Cheney²³ found no change in intrapulmonary shunt in hemodiluted dogs with oleic-acid induced lung injury; however, these investigators did not use a control group. In rabbits with left-lung atelectasis, acute hemodilution resulted in an increase in intrapulmonary shunt relative to controls followed over time;⁵ this effect is probably caused by attenuation of HPV, which in turn is caused by a relative excess of NO in association with a reduced sink in the form of hemoglobin.⁶ Studies in humans with acute respiratory failure of various causes suggest better gas exchange at lower hematocrit, but these studies are subject to the use of banked blood transfusion to increase hematocrit.²⁴⁻²⁶ The potential cardiovascular and inflammatory effects of autologous blood transfusion, in addition to the reduced 2,3-diphosphoglycerate in banked blood, makes these studies somewhat difficult to interpret.

A human form of chronic lung disease that approximates our model in terms of gas exchange abnormalities is chronic obstructive pulmonary disease (COPD). Chronic obstructive pulmonary disease is typified by the

presence of relatively little shunting and markedly abnormal \dot{V}_A/\dot{Q} matching.²⁷ In a study of patients with stable chronic obstructive pulmonary disease, transfusion from a hematocrit of approximately 30% to 37% was associated with a decrease in minute ventilation, a decrease in capillarized P_{O_2} , and an increase in capillarized P_{CO_2} .²⁸ The increase in P_{CO_2} was less than the associated decrease in minute variation ($r^2 = 0.36$), which suggests a possible improvement in gas exchange or alveolar ventilation after transfusion. However, interpretation of this study is difficult because of the lack of reported cardiac output, V_D/V_T , and $A-aP_{O_2}$ difference; in addition, the change in hematocrit occurred over a much higher range than in our rabbit model. The differing pathophysiologies of our model and chronic obstructive pulmonary disease in humans also makes direct comparisons of these data difficult.

In contrast to our previous findings in whole animals with normal lungs² and in isolated, perfused lungs,⁶ expired NO did not increase with decreasing hematocrit (fig. 2). We previously conjectured that anemia results in a reduced sink for NO, which is manifest as increased NO in the expired gas and, potentially, in effects on HPV and pulmonary blood flow distribution.^{5,6} The lack of an increase in expired NO with anemia in the current study is unexplained. We also noted an increase in $\dot{V}NO$ immediately after gas embolization. To our knowledge, no studies have investigated the effects of venous air embolization on lung NO production, although other types of experimental acute lung injury (sepsis-induced, oleic acid) are associated with evidence of increased NO production and excretion.²⁹⁻³² The relative stability of expired NO over time in the control group indicates that the effect of gas embolization on expired NO is immediate rather than cumulative and suggests a possible shear-stress-like effect of gas bubbles on the pulmonary endothelium.

Venous Gas Embolization, Anemia, and Pulmonary Blood Flow Distributions

In rabbits with normal lungs, we found that isovolemic anemia resulted in improved \dot{V}_A/\dot{Q} distribution in association with improved gas exchange.² The mechanism for this improvement in \dot{V}_A/\dot{Q} was unclear, although we also found a reduction in the D and increased spatial correlation of pulmonary blood flow distribution. These two findings suggest that anemia may result in greater uniformity of pulmonary blood flow. In the current study, however, we found no significant changes in either \dot{V}_A/\dot{Q} or pulmonary blood flow distribution, al-

though there was a slight trend toward more uniform pulmonary blood flow distribution, as measured by CV_Q , $Skewness_Q$ and flow along the y -axis (ventral-dorsal; table 3). The lack of significant improvement in pulmonary blood flow distribution is somewhat surprising given that one might expect anemia to have its greatest effect on pulmonary blood flow in the presence of vascular obstruction (gas embolization). It is possible that the resolution of our fluorescent microsphere methods is not sufficient to detect changes that may have occurred at a more microvascular level.

It is notable that changes in Pa_{O_2} over time can be explained in large part by changes in intrapulmonary shunting and SV_{O_2} ($r^2 = 0.60$). However, these observations do not provide a completely satisfying explanation for the observed improvement in Pa_{O_2} in anemic animals, given that significant changes in pulmonary blood flow distribution were not found. In addition, based on our previous work, anemia would be expected to result in an increase in Q_S/Q_T , probably secondary to an increase in the vasodilator compound NO and attenuation of HPV.^{5,6} However, in the current study, expired NO did not increase with hemodilution as expected. The lack of an increase in Q_S/Q_T with anemia in the current model is thus consistent with the observed changes in expired NO. We can only conjecture that anemia resulted in an unmeasured change in pulmonary blood flow distribution that led to an associated reduction in Q_S/Q_T in comparison with the control group.

Conclusions

Acute hemodilution results in improved oxygen exchange during venous gas embolization in rabbits, with the effect most pronounced to a hematocrit of approximately 15%. The mechanism for this improvement in gas exchange is unclear, but may be related to more uniform distribution of pulmonary blood flow caused by reduced blood viscosity and a reduction in intrapulmonary shunt. The clinical implication of this study is that anemia may not further impair gas exchange during pulmonary embolic syndromes, particularly if cardiac output is preserved.

Appendix: Methods for Calculation of Fractal Dimension of Pulmonary Blood Flow Distribution

The fractal dimension statistic (D) is related to the degree of local correlation of flow among lung pieces. A large value of D indicates a

low degree of local spatial correlation; *i.e.*, flows to neighboring pieces are relatively dissimilar. Conversely, a small value of D indicates a high degree of local correlation; *i.e.*, flows to neighboring pieces are relatively similar. An attractive feature of the fractal dimension statistic D is that it is independent of piece size. The statistic D supplements and provides different information than the coefficient of variation (CV), which depends on a specific piece size. Empirically, it is possible to have a large or small value of CV with a large or small value of D. Thus, a useful pair of statistics within an experiment is the CV at piece size = 1 as a measure of heterogeneity, along with D as a measure of local spatial correlation.

Fractal dimension is calculated from the CV of blood flow to individual pieces, using a range of piece sizes.³ By combining neighboring core lung pieces into a conglomerate piece of a given size (based on multiples of the initial piece size) the CV of blood flow could be calculated as if the lung had been divided into larger pieces. Conglomerate piece sizes of 2, 3, 4, 6, 8, 12, 16, 24, 32, 48, and 64 were constructed as follows: A central piece was chosen at random from all available pieces, then neighboring pieces were chosen until the desired conglomerate size was reached. Individual pieces assigned to a conglomerate were then flagged as unavailable. The process was repeated, choosing another central piece at random from the remaining available pieces. If a conglomerate could not be constructed because of unavailability of neighboring pieces, the central piece was abandoned and another was chosen. This was repeated until the lung was divided into as many conglomerate pieces as possible. Conglomerates were restricted to lie entirely within the left or the right lung, but were not restricted to be entirely within lobes. For a given conglomerate piece size, the CV will vary randomly, depending on which individual lung pieces were assigned to which conglomerates. We therefore repeated the algorithm for dividing the lung into larger conglomerate pieces. For conglomerates of size n , we repeated the process \sqrt{n} times (rounding up to the next integer value for noninteger square roots). Thus, for conglomerates of size 64, we repeated the algorithm eight times, obtaining eight CVs. We used the mean of the logarithm of the eight CVs for regression modeling to obtain D, used the standard deviation of the logarithm of the eight CVs for plotting error bars, and used the total number of conglomerate pieces for all eight repetitions as the regression weight at piece size 64. $\log(CV)$ was plotted against $\log(\text{piece size})$, and a regression line was obtained using weighted regression analysis. D was calculated as $(1 - \text{slope})$, where slope was obtained from the regression line fitted to the $\log(CV)$ versus $\log(\text{piece-size})$ data. A larger D indicates less local spatial correlation among piece flows.

References

1. Deem S, Alberts MK, Bishop MJ, Bidani A, Swenson ER: CO₂ transport in normovolemic anemia: Complete compensation and stability of blood CO₂ tensions. *J Appl Physiol* 1997; 83(1):240-6
2. Deem S, Hedges RG, McKinney S, Polissar NL, Alberts MK, Swenson ER: Mechanisms of improvement in pulmonary gas exchange during isovolemic hemodilution. *J Appl Physiol* 1999; 87:132-41
3. Glenny RW, Robertson HT: Fractal properties of pulmonary blood flow: characterization of spatial heterogeneity. *J Appl Physiol* 1990; 69(2):532-45
4. Glenny RE, Robertson HT, Yamashiro S, Bassingthwaite JB: Applications of fractal analysis to physiology. *J Appl Physiol* 1991; 70(6):2351-67

5. Deem S, Bishop MJ, Alberts MK: Effect of anemia on intrapulmonary shunt during atelectasis in rabbits. *J Appl Physiol* 1995; 79(6): 1951-7
6. Deem S, Alberts MK, Hedges RG, Swenson ER, Bishop MJ: The interaction between red blood cells and hypoxic pulmonary vasoconstriction: The role of nitric oxide and adenosine. *Am J Respir Crit Care Med* 1998; 157:1181-6
7. Hlastala MP, Robertson HT, Ross BK: Gas exchange abnormalities produced by venous gas emboli. *Res Physiol* 1979; 36:1-17
8. Wagner PD, Naumann PF, Lavaruso RB: Simultaneous measurement by eight foreign gases in blood by gas chromatography. *J Appl Physiol* 1974; 36:600-5
9. Hlastala MP: Multiple inert gas elimination technique. *J Appl Physiol* 1984; 56:1-7
10. Isoyama T, Sato T, Tanaka J, Shatney CH: Measurement of cardiac output in small animals by aortic thermodilution. *J Surg Res* 1982; 33:170-6
11. Wanless RB, Anand IS, Poole-Wilson PA, Harris P: Haemodynamic and regional blood flow changes after acute pulmonary microembolism in conscious rabbits. *Cardiovasc Res* 1988; 22:31-6
12. Warren DJ, Ledingham JGG: Cardiac output in the conscious rabbit: An analysis of the thermodilution technique. *J Appl Physiol* 1974; 36:246-51
13. Wagner PD, Saltzman HA, West JB: Measurement of continuous distributions of ventilation-perfusion ratios: Theory. *J Appl Physiol* 1974; 36:588-99
14. Buckberg GD, Luck JC, Payne DB, Hoffman JI, Archie JP, Fixler EE: Some sources of error in measuring regional blood flow with radioactive microspheres. *J Appl Physiol* 1971; 31:598-604
15. Glenny RW, Bernard S, Brinkley M: Validation of fluorescent-labeled microspheres for measurement of regional organ perfusion. *J Appl Physiol* 1993; 74:2585-97
16. Hlastala MP, Bernard SL, Erickson HH, Fedde MR, Gaughan EM, McMurphy R, Emery MJ, Polissar N, Glenny RW: Pulmonary blood flow distribution in standing horses is not dominated by gravity. *J Appl Physiol* 1996; 81(3):1051-61
17. Glenny RW, Lamm WJ, Albert RK, Robertson HT: Gravity is a minor determinant of pulmonary blood flow distribution. *J Appl Physiol* 1997; 73(5):620-9
18. Glenny RW, Polissar NL, McKinney S, Robertson HT: Temporal heterogeneity of regional pulmonary perfusion is spatially clustered. *J Appl Physiol* 1995; 79(3):986-1001
19. Orebaugh SL: Venous air embolism: Clinical and experimental considerations. *Crit Care Med* 1992; 20(8):1169-77
20. Moosavi H, Utell MJ, Hyde RW, Fahey PJ, Peterson BT, Donnelly J, Jenson KD: Lung ultrastructure in noncardiogenic pulmonary edema induced by air embolization in dogs. *Lab Invest* 1981; 45(5):456-64
21. Ohkuda K, Nakahara K, Binder A, Staub NC: Venous air emboli in sheep: reversible increase in lung microvascular permeability. *J Appl Physiol: Respirat Environ Exercise Physiol* 1981; 51(4):887-94
22. Peterson BT, Grauer SE, Hyde RW, Ortiz C, Moosavi H, Utell MJ: Response of pulmonary veins to increased intracranial pressure and pulmonary air embolization. *J Appl Physiol: Respir Environ Exercise Physiol* 1980; 48:957-64
23. Bishop MJ, Cheney FW: Effects of hemodilution during pulmonary edema in dogs. *Ann Surg* 1983; 198(1):96-101
24. Fortune JB, Feustel PJ, Saifi J, Stratton HH, Newell JC, Shah KM: Influence of hematocrit on cardiopulmonary function after acute hemorrhage. *J Trauma* 1987; 27(3):243-9
25. Kahn RC, Zaroulis C, Goetz W, Howland WS: Hemodynamic oxygen transport and 2,3-diphosphoglycerate changes after transfusion of patients in acute respiratory failure. *Intensive Care Med* 1986; 12: 22-5
26. Steffes CP, Bender JS, Levison MA: Blood transfusion and oxygen consumption in surgical sepsis. *Crit Care Med* 1991; 19(4):512-7
27. Agusti AGN, Barbera JA: Contribution of multiple inert gas elimination technique to pulmonary medicine: II. Chronic pulmonary diseases: Chronic obstructive disease and idiopathic pulmonary fibrosis. *Thorax* 1994; 49:924-32
28. Schönhofer B, Wenzel M, Geibel M, Kohler D: Blood transfusion and lung function in chronically anemic patients with severe chronic obstructive pulmonary disease. *Crit Care Med* 1998; 26(11):1824-8
29. Schutte H, Mayer K, Gessler T, Ruhl M, Schlaudraff J, Gurger H, Seeger W, Grimminger F: Nitric oxide biosynthesis in an exotoxin-induced septic lung model: Role of cNOS and impact on pulmonary hemodynamics. *Am J Respir Crit Care Med* 1998; 157:498-504
30. Stewart TE, Valenza F, Ribeiro SP, Wener AD, Bolgyesi G, Mullen JB, Slutsky AS: Increased nitric oxide in exhaled gas as an early marker of lung inflammation in a model of sepsis. *Am J Respir Crit Care Med* 1995; 151(3):713-8
31. Leeman M, De-Beyl VZ, Gilbert E, M'elot C, Naeije R: Is nitric oxide released in oleic acid lung injury? *J Appl Physiol* 1993; 74(2): 650-4
32. Aaron SD, Valenza F, Volgyesi G, Mullen JB, Slutsky AS, Stewart TE: Inhibition of exhaled nitric oxide production during sepsis does not prevent lung inflammation. *Crit Care Med* 1998; 26(2):309-14